

THE SUBSURFACE ELECTRICAL CONDUCTIVITY AND THE ATTENUATION OF CODA WAVES AT LAS TRES VÍRGENES GEOTHERMAL FIELD IN BAJA CALIFORNIA SUR, MÉXICO.

José M. Romo, Victor Wong, Carlos Flores and Rogelio Vázquez
CICESE, División de Ciencias de la Tierra, Ensenada B.C., México

Keywords: geophysics, electrical conductivity, seismic wave attenuation, Las Tres Vírgenes, México.

ABSTRACT

The presence of highly fractured rocks with fluids at high temperature can substantially increase the attenuation of the seismic waves as well as the electrical conductivity. The data collected in Las Tres Vírgenes geothermal field by a seismological network, as well as by multiple geophysical surveys including: magnetotellurics (MT), transient electromagnetic (TDEM) and d.c.-resistivity vertical soundings (Schlumberger), allowed to outline the zones where the electrical conductivity and the attenuation of elastic waves are unusually high. The seismic activity was registered during 23 days by a portable array consisting of thirteen digital stations. We used 26 local events with magnitude ranging between 0 and 3.0 to estimate the attenuation associated to underground volumes traversed by different ray paths. The quality factor Q_c was estimated in the frequency range from 6 to 24 Hz, using the coda waves and a single scattering model. We use the magnetotelluric responses measured in 90 sites to estimate the subsurface distribution of the electrical conductivity in a depth range from 0 to 3 km. The results suggest the presence of a highly attenuating and conductive zone along El Azufre Canyon: the boundary between Las Tres Vírgenes complex and El Aguajito complex. In that zone we found an abnormally strong reduction of the quality factor Q_c as the frequency decreases, causing attenuation values 3 or 4 times larger than the values estimated at the rest of the area. Likewise, in the same region we found electrical resistivity lower than $5 \Omega\text{-m}$ at depths ranging from 250 to 2500 m. Both results are in agreement with the geological knowledge that there are intense rock fracturing and high temperatures at depth (240°C at 1142 m. in well LV-2).

1. INTRODUCTION

In 1983 the Comisión Federal de Electricidad (CFE) initiated the exploration of Las Tres Vírgenes prospect, where recent volcanism and surface hydrothermal manifestations were known (Lira et al., 1983). The area is located at $112^\circ 30'$ longitude W and $27^\circ 30'$ latitude N, in the central portion of the Baja California Península, in México (Figure 1).

The exploration studies have included geology, geophysics, hydrology and geochemistry. The principal results have been recently summarized in López et al. (1995), Arredondo (1995), López (1998), García and González (1998), Bigurra (1998), and Palma (1998).

The area is located in the Santa Rosalía Basin, a Plio-Quaternary depression tectonically related with the opening of the Gulf of California (~10 My b. p.). The Cenozoic extensional regime originated a fault system oriented NW-SE

facilitating the emplacement of eruptive centers. Three major volcanic centers formed during the Cenozoic: La Reforma Caldera (~ 6.5 My b. p.), El Aguajito Complex (~ 6.5 My b. p.) and Las Tres Vírgenes Complex (~ 0.44 My b. p.), the last one comprised of La Virgen, El Viejo-El Partido and El Azufre volcanoes. In addition to the NW-SE system there are evidence of younger NE-SW and N-S fault systems, probably related to the current transcurrent tectonic regime.

The oldest lithologic unit found at 1000 m depth is a granodiorite (91-84 My b. p.) that is related to a peninsular batholith and has been taken as the basement in the area. Overlaying the basement there is a ~750 m-thick volcano-sedimentary sequence (Comondú Group) followed by a sequence of andesitic lava flows and pyroclastic products (Fm. Santa Lucía) with variable thickness. The Santa Rosalía basin is filled up with shallow-water marine deposits characterized by a fossiliferous sandstone. At the top of the above sequence there are a variety of pyroclastic products related to the different stages of the Cenozoic volcanism.

The information provided by the exploration works suggest that there exist geothermal fluids at depth (~1200 m) with high pressure (~120 bar) and temperature over 250°, in some localized zones of the granodioritic basement where the rock permeability has been increased by intense fracturing. Four production and two reinjection wells had been drilled up to 1998. The developing of the field is actually in progress, the short term goal is to install two 5 MW condensing units. With the available information is possible to project a generation of 25 MW in the long term (Sánchez-Velasco, 1996). The success of this project will render possible to supply clean and cheap energy, in an area where mining, fishery and tourism are growing industries and where the preservation of a natural reserve is an important issue.

2. ELECTRICAL CONDUCTIVITY

In 1984 a d.c.-resistivity survey (Ballina and Herrera, 1984) was carried out to delineate subsurface electrical conductivity anomalies of geothermal interest. Three conductive zones aligned along the El Azufre Canyon were reported: Cerro Blanco, las Víboras-La Puerta and Cuevegel.

In 1992 the first stage of a MT survey consisting of 20 sites was completed (Vázquez et al., 1992). The investigation continued in 1994 with a second survey, this time including 70 MT sites complemented with 55 TDEM soundings (Romo et al., 1994). The sites measured in both surveys are distributed on an approximated area of 400 km^2 (figure 2). This data set is used in this work to investigate the subsurface electrical conductivity, as well as 44 Schlumberger sites from Ballina and Herrera, (1984).

The Schlumberger and TDEM measurements were used to constrain the conductivity at shallow depths (from 0 to

500 m), as a means of correcting the distortion on the MT response caused by conductivity variations in this interval. They were interpreted in terms of layers and the magnetotelluric response of the layered models was used to correct the measured MT curves. Most of the models consist of a two-layer sequence resistor-conductor laying on a resistive basement ($> 500 \Omega\text{-m}$). The first layer is about 160 m thick with a resistivity range from 200 to 1000 $\Omega\text{-m}$. The conductive layer has 5 $\Omega\text{-m}$ in average and it is 350 m thick. The zones where the thickness and resistivity of the first layer decreases correspond with the zones where hydrothermal alteration has been mapped on the surface.

The electromagnetic fields were registered for a frequency band from .005 to 50 Hz and used to estimate the MT response with a remote reference technique. A qualitative analysis of the responses indicates that, at frequencies below 1 Hz, the electrical current is flowing preferentially along a NW-SE direction, while at higher frequencies there is no preferential direction for the current flow. In general, the apparent resistivity curves for both polarization modes are coincident in a frequency band from 1 to 50 Hz, resembling the response of a one-dimensional (1-D) shallow structure. The 1-D models obtained with these data show a conductive layer (1-5 $\Omega\text{-m}$), at depths between 250 and 750 m. This feature alone explains most of the responses at the high frequency band (1-50 Hz).

At lower frequencies we have a different behavior: the electric field is disturbed by lateral variations of conductivity, as a consequence the apparent resistivity curves separate and the 1-D models are useless. Accordingly the simulation was made in terms of two-dimensional (2-D) models. Nine profiles were selected to be modeled, seven of them oriented NE-SW and two more NW-SE. Here we show the models obtained for two profiles: Line I-NE (figure 3) and Line I-NW (figure 4).

In the model shown in figure 3, the thickness of the conductive zone ($< 5 \Omega\text{-m}$) detected under sites s12, s11 and s04, changes from 500 m beneath s12 to more than 1200 m beneath sites s11 and s04. This zone corresponds with the production interval of wells LV-2 and LV-3/4. Considering the distribution of resistivity less than 20 $\Omega\text{-m}$, a graben structure can be outlined between sites s12 and s10. The southwestern limit of the structure produce the strong lateral contrast found at depth below s12, and could correspond to the El Partido fault. The 1 $\Omega\text{-m}$ vertical conductor under s04 is the northeastern limit of the graben and can be associated with El Azufre fault. This graben constitutes one of the prominent structures of the area. A notable fact is the different conductivity found at each flank of the graben: it seems to implicate that while El Azufre fault zone is highly permeable, the El Partido fault zone is not.

The resistivity model for Line I-NW (figure 4) shows a simpler subsurface image. The conductive zone ($< 5 \Omega\text{-m}$) extends horizontally between site s85 and s45, its thickness is greater below s12 and decreases toward both sides of the section. As the case described above, the thickness change of the conductive zone beneath s12 could be related with a geologic structure, this time belonging to the NE-SW fault system. However, in this case a structural feature is difficult to postulate, because the weaker conductivity contrasts as well as the insufficient number of sites along the line. The stronger lateral contrast found at depth between site s85 and site s69 seems to provide better evidence to postulate a fault with a step of 1000 m at basement level.

3. SEISMICITY AND CODA WAVE ATTENUATION

From May to October 1992, Wong and Munguía (1992) registered more than 2000 seismic events with S-P time of less than 3 s and magnitude ranging between 1 and 3. The recurrence of swarm-like sequences suggested that the stress in this area is highly inhomogeneous.

In 1993 CFE installed a permanent digital network in order to monitor the intense seismic activity for exploration purposes. The net consists of six digital stations with three-component recording. The analysis of four months of recording (Munguía and Wong, 1993, 1995) shows that the epicenters are spatially clustered along the volcanic structures and toward the southeast of the network. Duration magnitude range from 1.0 to 4.0, the larger located in the Gulf of California. The composite focal mechanism solutions determined for a group of selected events, range between strike-slip and normal type. Most of the focal solutions show oblique faults, combining dip-slip and strike-slip. The variability of the focal mechanisms reflects the structural complexity of the zone.

The seismic data analyzed in this study were recorded by a portable array of thirteen stations deployed in the area in October 1993. The instrumentation was composed of six analog stations with a single vertical component, and seven digital stations with three components (figure 5). An absolute time basis was available for both analog and digital stations. The portable network operated for 23 days. During this period, 257 microearthquakes were located. The epicentral distribution (figure 5) shows that the activity concentrates on El Aguajito complex, on the volcanic chain and along the southeastern section of La Virgen fault. The focal depth range from 0 to 10 km: the shallow events are located on the volcanic chain and on El Aguajito, while the deeper ones are located along the El Azufre Canyon.

In this work we analyze the coda wave of the horizontal components of 26 microearthquakes that were recorded at least on five digital stations. We use these data to study the attenuation associated to different ray paths that traversed the volcanic volumes. The hypocentral locations were reported by Wong and Munguía (submitted to publication). The duration magnitude range from 1.0 to 3.0 and the focal depths between 3.0 and 6.0 km. We used a single scattering model based on the early coda of local earthquakes (Sato, 1977), to estimate the quality factor Q (Q_c). An averaged estimate $\langle Q_c \rangle$ was obtained at each station for a frequency band from 6 to 24 Hz.

The events were separated into three groups according to their epicentral location. The northeast group corresponds to events located beneath the El Aguajito complex, the central group corresponds to events located along the volcanic chain (El Viejo, El Azufre and La Virgen volcanoes) and the southeast group corresponds to events located along the southeastern section of the La Virgen fault. The $\langle Q_c \rangle$ vs. frequency response was estimated for each group at seven stations (E1, E3, E6, E10, E12, E13 and E14).

The results are shown in figure 6 (the error bars indicate one standard deviation). From a first look it is evident that station E1 shows the same anomalous behavior for each epicentral region. At this station the value of Q_c reduces abruptly as frequency decreases, e.g. the value at 6 Hz is a factor of 4 or 5 lower than in the value at the other stations. The responses at

the other six stations are comparable each other, with the larger differences at low frequencies. All of them show a moderate Q_c reduction as frequency decreases, a typical result reported in other volcanic areas (Chouet, 1976; Del Pezzo et al., 1987; De Natale et al., 1987; Zuñiga and Díaz, 1994).

The anomalous behavior of station E1 can be explained by a local distortion produced within a volume close to the site. It is possible that the estimated Q_c does not represent a measure of the total attenuation, but one of the intrinsic absorption. Therefore, as is pointed out by Aki (1980) and Gao (1992), it should be very sensitive to temperature, to the liquid contained in the cracks, and to the flow between adjacent interacting cracks near the station.

On the other hand, the response of a given station (E1 included) is comparable between different regions, in spite of the fact that they sampled different portions of the crust. This behavior of Q_c suggests that the elastic properties within the different volumes illuminated by each epicentral region were averaged in such a way that their responses become undistinguishable.

4. CONCLUSIONS

The magnetotelluric models show a conductive zone ($<5 \Omega\text{-m}$), at depths between 250 and 750 m, probably related to the permeable components of the Santa Lucía Fm. and Comondú Group. At Line I-NE (figure 3) the thickness of the conductive zone under sites s12, s11 and s04 changes from 500 m beneath s12 to more than 1200 m beneath s11 and s04. This corresponds with the production interval of wells LV-2 and LV-3/4

On Line I-NE (figure 3) a graben structure can be outlined between sites s12 and s10, based on the distribution of resistivity smaller than $20 \Omega\text{-m}$. The southwestern limit of the structure produce the strong lateral contrast found at depth below s12, and could correspond to the El Partido fault. The $1 \Omega\text{-m}$ vertical conductor under s04 is the northeastern limit of the graben and can be associated with El Azufre fault. A notable fact is the different conductivity found at each flank of the graben: it seems to implicate that while El Azufre fault zone is highly permeable, the El Partido fault zone is not.

The resistivity model for Line I-NW (figure 4) shows the conductive zone ($<5\Omega\text{-m}$) extending horizontally between site s85 and s45, its thickness is greater below s12 and decreases toward both sides of the section. In this case a structural feature is difficult to postulate, because the weaker conductivity contrasts as well as the insufficient number of sites along the line. The stronger lateral contrast found at depth between site s85 and site s69 seems to provide better evidence to postulate a fault with a step of 1000 m at basement level.

The comparable Q_c responses obtained at all the stations, for different epicentral regions, suggest that they are not sensitive to differences in the elastic properties of large subsurface volumes illuminated by each group of ray paths. Otherwise, the anomalous values obtained in station E1 for the three groups of ray paths, suggest that the responses are sensitive to differences of elastic properties in the volume directly beneath the station.

It is possible that the Q_c values estimated on the basis of the single scattering theory do not represent a measure of the total attenuation, but one of the intrinsic absorption. Therefore, it should be very sensitive to temperature, to the liquid contained in the cracks, and to the flow between adjacent interacting cracks near the station.

The moderated frequency dependence obtained in six of the stations is a typical result reported in other volcanic areas, where it was interpreted as indicative of magma and/or high temperatures at depth.

The presence of a highly attenuating and conductive zone has been observed along El Azufre Fault: a major geologic structure that possibly affects the basement. In that zone we found an abnormally strong reduction of the quality factor Q_c as the frequency decreases, causing attenuation values 3 or 4 times larger than the values estimated at the rest of the area. Likewise, at the same region we found electrical resistivity lower than $5 \Omega\text{-m}$ at depths ranging from 250 to 2500 m. Both results are in agreement with the geological knowledge that there are intense rock fracturing and high temperatures at depth (240°C at 1142 m. in well LV-2).

ACKNOWLEDGMENTS

This work was originated after two research projects carried out at CICESE under contract for CFE's Gerencia de Proyectos Geotermoelectrivos (GPG). The authors appreciate the authorization granted by Dr. Gerardo Hiriart, GPG manager, to publish these results.

The authors gratefully appreciate the participation of the CICESE's personnel involved in the fieldwork as well as in the data processing and interpretation of both the seismology and magnetotelluric projects. We also appreciate the support and cooperation provided by CFE's personnel, especially by Francisco Arellano and Saúl Venegas.

Tamks are also extended to Humberto Benítez who help us in the preparation of the manuscript figures.

REFERENCES

- Aki, K. (1980). Attenuation of shear-waves in the lithosphere for frequencies from 0.05 to 25 Hz. *Phys. Earth Planet. Inter.*, Vol. 21(?), pp. 50- 60.
- Arredondo, J. (1995). *Reinterpretación gravimétrica a detalle en la zona de Los pozos LV-1, LV-2 y LV-3 en el campo geotérmico de Las Tres Virgenes*, B. C. S., Intern. Rep. 32/95, GPG-CFE, 18 pp.
- Ballina, H. and Herrera F. (1984). *Estudio geofísico en la zona geotérmica de Las Tres Virgenes*, B. C. S., Intern. Rep. 32/95, GPG-CFE, 28 pp.
- Bigurra, E. (1998). Análisis geoelectrónico de la zona geotérmica de Las Tres Virgenes, B.C.S., México. *Geotermia*, Vol. 14(1), pp. 33-41.
- Chouet, B. (1976). *Source, scattering and attenuation effects on high frequency seismic waves*. Ph.D. thesis, Massachusetts Institute of Technology, Cambridge, Massachusetts.

Del Pezzo, E., Gresta, E., Patané, G., Patané, D., and Scarella, G. (1987). Attenuation of short period seismic waves at Etna as compared to other volcanic areas, *Pageoph*, 125, pp. 1039-1050.

De Natale, G., Iannaccone, G., Martini, M., and Zollo, A. (1987). Seismic sources and attenuation properties at the Campi Flegrei volcanic area, *Pageoph*, 125, pp. 883-917.

Gao, L.S., (1992). *Physical meaning of the coda envelopes*, In: *Volcanic Seismology*, In: *Proceedings in Volcanology* (I.A.V.C.E.I.), P. Gasparini, R. Scarpa, and K. Aki, (Eds.), Vol. 3, Springer-Verlag, New York, pp. 391-403.

Gracia G., and González, M. (1998). Síntesis de los estudios de gravimetría, magnetometría y termometría en la zona geotérmica de las Tres Vírgenes, B.C.S., México, *Geotermia*, Vol. 14(1), pp. 15-32.

Lira, H., Ramirez, G., Herrera, J., and Vargas, H. (1983). *Estudio geológico a semidetalle de la zona geotérmica de las Tres Vírgenes*, B. C. S., Intern. Rep. 30/83, GPG-CFE, 33 pp.

López, A., Garcia G., and Arellano F.J. (1995). Geothermal exploration at Las Tres Vírgenes, B.C.S., México, *Proceeding of the 1995 World Geoth. Congress*, (I.G.A), Vol. 2, pp. 707-712,

López, A. (1998). Síntesis geológica de la zona geotérmica de Las Tres Vírgenes, B.C.S., México, *Geotermia*, Vol. 14(1), pp. 3-14.

Munguía, L., and Wong, V. (1993). *Analisis e interpretación de la información sísmica digital registrada en el campo geotérmico de Tres Vírgenes, B. C. S. en el período Febrero-Mayo de 1993*, Intern. Rep., Contract CLS-GPG-3013-93/CFE-CICESE, GPG-CFE, 128 pp.

Munguía, L., and Wong, V. (1995). *Estudio de sismicidad en la zona geotérmica las Tres Vírgenes, Baja California Sur*, In: *La sismología en México: 10 años después del temblor de Michoacán del 19 de Septiembre de 1985 (M=8.1)*, (U.G.M.), Medina-Martínez, F., Delgado-Argote, L.A., and Suárez-Reynoso, G., (Eds.), Monografía No. 2, pp. 212-228.

Palma, S.H. (1998). Modelado de datos magnetotelúricos en el campo geotérmico de Las Tres Vírgenes, B.C.S., México, *Geotermia*, Vol. 14(1), pp. 43-53.

Romo, J. M., Flores, C., Vega, R., Esparza F., and Gómez, E. (1994). *Estudio magnetotelúrico en el área geotérmica Tres Vírgenes-Aguajito, B.C.S.: Informe de Interpretación*, Intern. Rep., Contract CLS-GPG-4003-94/CFE-CICESE, GPG-CFE, 527 pp.

Sánchez-Velazco, R. (1996). Aspectos Generales del Proyecto Geotérmico de las Tres Vírgenes, B. C. S., México, *Geotermia*, 12, pp. 115-124.

Sato, H. (1977). Energy propagation including scattering effects: single isotropic scattering approximation, *J. Phys. Earth*, 25, pp. 27-41.

Vázquez, R., Vega, R., Herrera, F., and López, A. (1992). *Evaluación con métodos electromagnéticos del campo geotérmico de Tres Vírgenes*, B. C. S., Primera etapa, Intern.

Rep., Contract CLS-GPG-003-94/CFE-CICESE, GPG-CFE, 175 pp.

Wong, V., and Munguía, L. (1992). *Monitoreo sísmico del área geotérmica de Tres Vírgenes, Baja California Sur*, Intern. Rep., Contract CLS-CPG-3011-92/CFE-CICESE, GPG-CFE, 16 pp.

Wong, V., and Munguía, L. (submitted). Seismic studies and focal mechanisms determination at Las Tres Vírgenes volcanic area, B.C.S., México.

Zuñiga, F.R., and Díaz, L.E. (1994). Coda attenuation in the area of El Chichón volcano, Chiapas, México, *Tectonophysics*, 234, pp. 247-258.

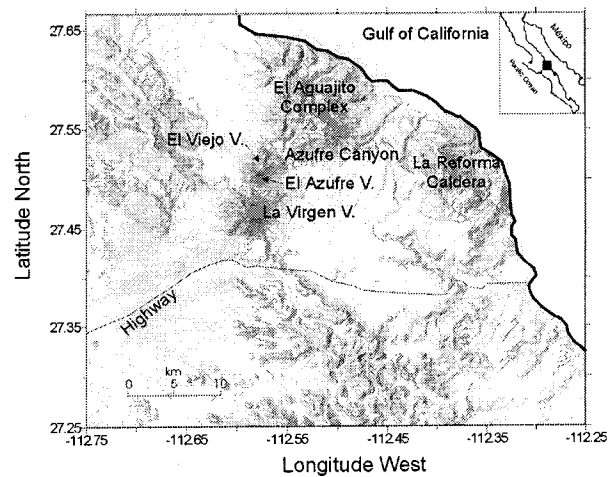


Figure 1. Location of Las Tres Vírgenes Geothermal project in Baja California Sur, México.

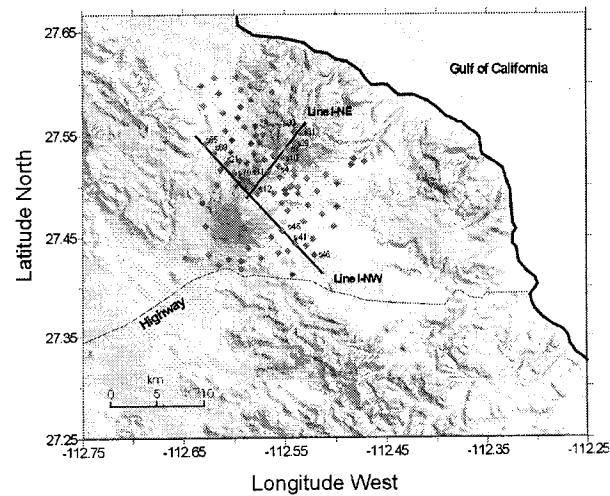


Figure 2. Magnetotelluric sites and modeled lines.

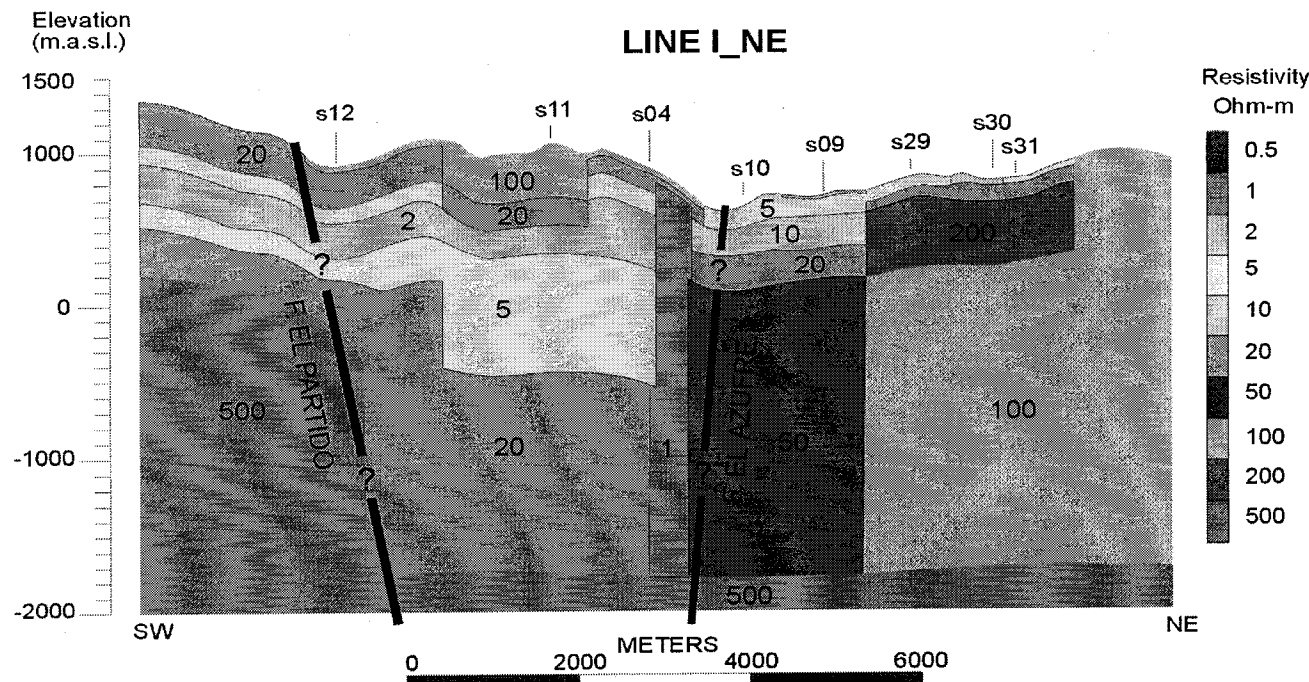


Figure 3. Subsurface resistivity model along line I-NE

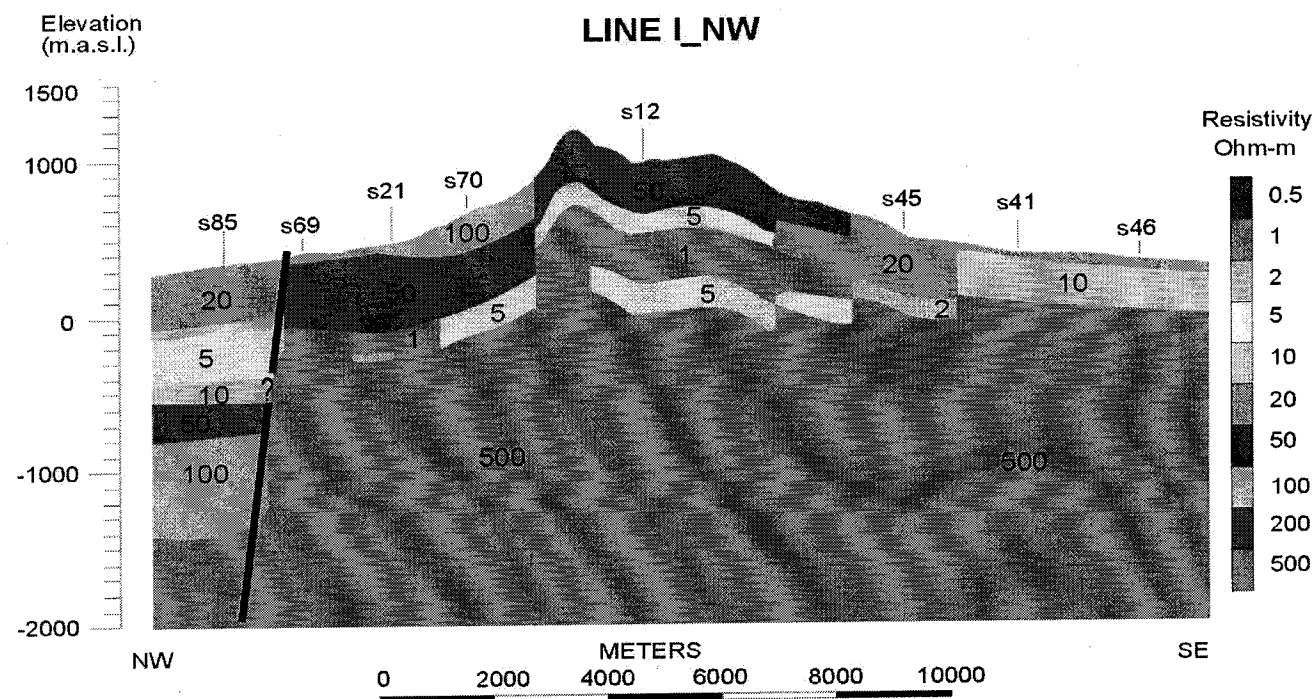


Figure 4. Subsurface resistivity model along line I-NW.

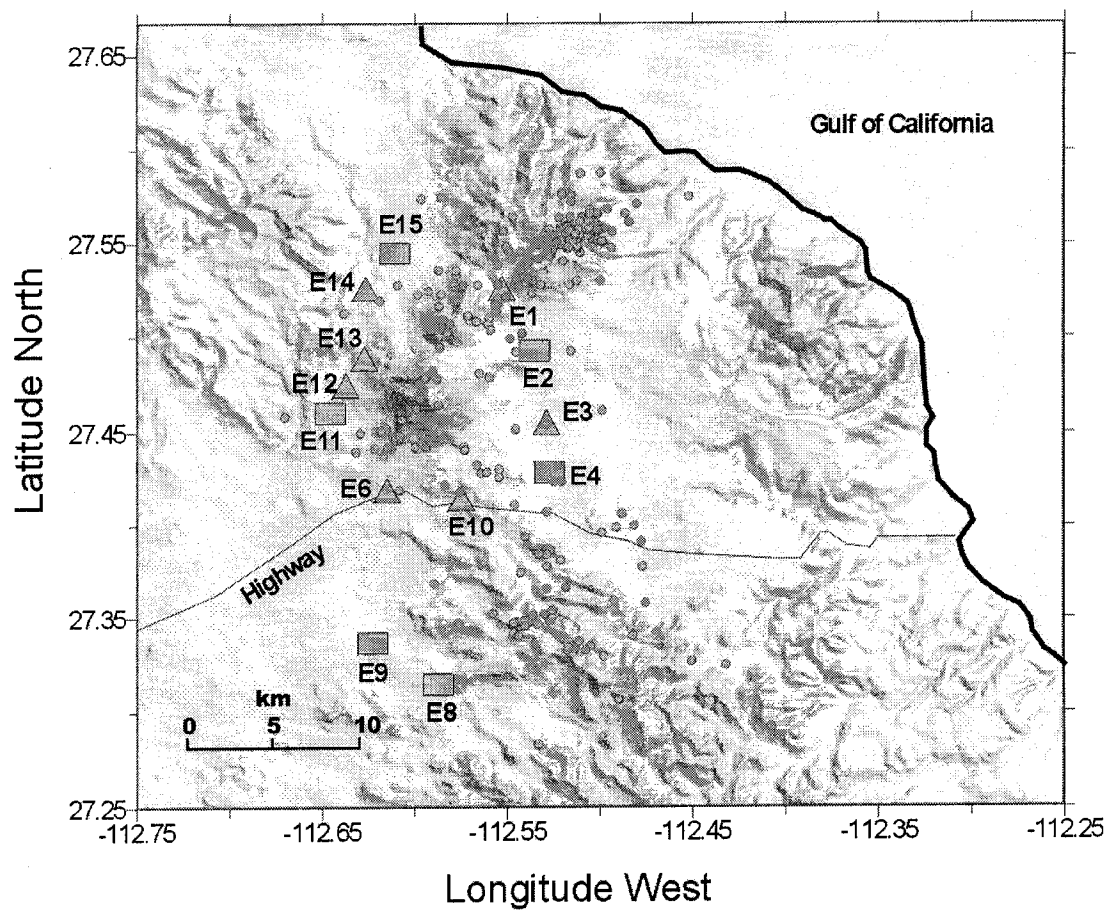


Figure 5. Seismic network and location of epicenters. 3-component digital stations 1-component analog stations epicentral locations.

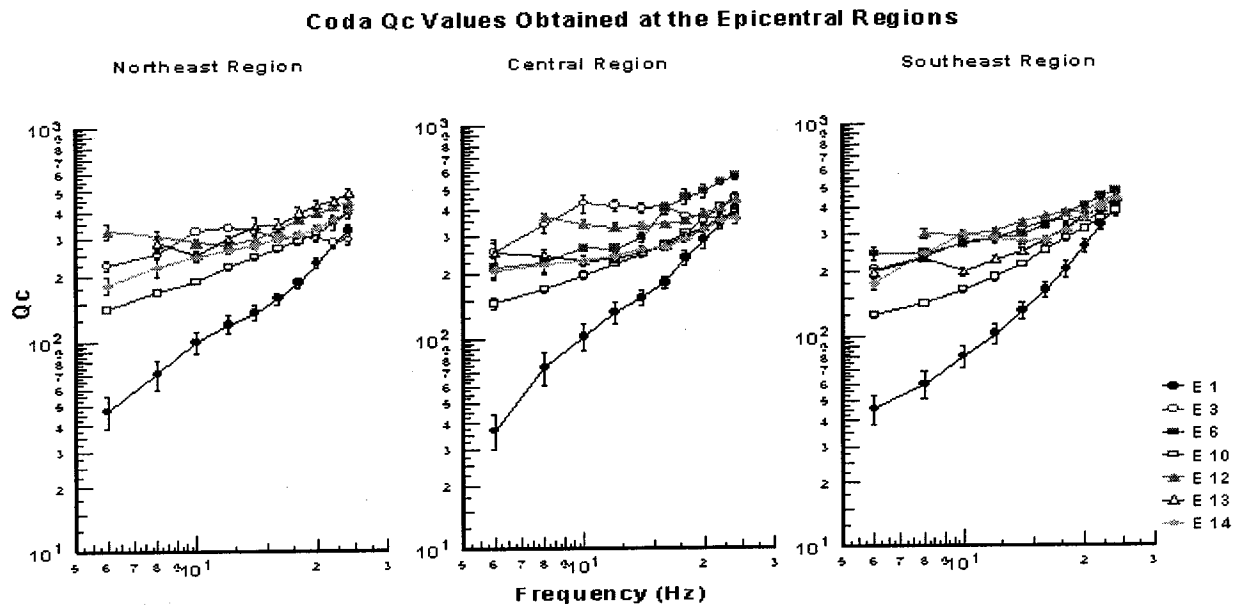


Figure 6. Frequency response of the quality factor Q_c estimated for different ray path regions at seven digital stations.